

Intrinsic spin-density-wave magnetism in Cu-Mn alloys

F. J. Lamelas* and S. A. Werner

Department of Physics, The University of Missouri, Columbia, Missouri 65211

S. M. Shapiro

Department of Physics, Brookhaven National Laboratory, Upton, New York 11973

J. A. Mydosh

Kammerlingh Onnes Laboratory, Rijksuniversiteit, 2300 RA Leiden, The Netherlands

(Received 23 May 1994)

Elastic neutron-scattering measurements on two samples of Cu alloyed with 1.3% Mn and 0.55% Mn show that the spin-density-wave (SDW) features found in more concentrated alloys persist in the limit of very dilute alloys. These features consist of temperature-dependent incommensurate peaks in magnetic neutron scattering, with positions and strengths which are fully consistent with those in the concentrated alloys. The implications of these measurements are twofold. First, it is clear from our data that SDW magnetic ordering occurs across the entire range of Cu-Mn alloys which have typically been interpreted as spin glasses. Second, the more fundamental significance of this work is the suggestion *via* extrapolation that a peak in the magnetic susceptibility $\chi(\mathbf{q})$ occurs in *pure copper*, at a value of q given by the Fermi-surface diameter $2k_F$.

In condensed-matter physics, structural measurements can be considered fundamental in that all theories and experiments must be consistent with the structural data. For magnetic materials, the most powerful structural probe available is neutron scattering. However, in the study of Cu-Mn spin glasses, crucial neutron-scattering results¹ were obtained rather late in the development of the field² and thus their impact has been limited. This situation has arisen because of the relative weakness of the scattering associated with spin ordering, and also because the interpretation of the neutron data has evolved slowly over the past decade, aided, to a significant degree, by new theoretical developments.^{3,4} In this paper we discuss a Cu 0.55% Mn crystal which represents a probable limit in the composition which is accessible with current neutron-scattering sources and techniques. The current data, together with earlier measurements on more concentrated alloys, bracket the range of compositions which has formed the subject of intensive spin-glass studies.

The neutron data form a picture which is rather at odds with the standard view⁵ of the nature of a spin glass. Taken as a whole, the scattering measurements suggest that the most straightforward interpretation of Cu-Mn alloys is that of a spin-density-wave (SDW) antiferromagnet (AFM).⁶ However, no long-range order is developed in this AFM, as evidenced by the uniform observation of SDW peak widths corresponding to domains which are only ten fcc unit cells in extent. Nevertheless, broadened peaks are not necessarily due to incomplete ordering, but may instead reflect the intrinsic nature of antiferromagnetism in Cu alloys.⁴ In our view, SDW's are stabilized as a consequence of a peak in the susceptibility $\chi(\mathbf{q})$ at $q = 2k_F$; the characteristic size of correlated-spin domains is governed by the width of the peak in

$\chi(\mathbf{q})$. Thus, the neutron-scattering data for dilute alloys serve as a probe of the wave-vector-dependent magnetic susceptibility of pure copper metal.

Our measurements were performed on samples prepared by standard methods in Leiden. The first crystal, with a composition of Cu 1.3 at. % Mn \pm 0.2% was grown by single-pass zone melting in a graphite crucible under Ar. A second sample, of composition Cu 0.55 at. % Mn \pm 0.07%, was prepared using the Czochralski technique. This crystal was annealed at 950 °C to remove strains and promote homogeneity. The mosaics of the samples were 1.2° for 1.3% Mn and 0.6° for 0.55% Mn. The samples were cylindrical, approximately 50 mm long and 12 mm in diameter. Neutron-scattering measurements were carried out on the triple-axis spectrometer H7 at the High-Flux Beam Reactor (HFBR) at Brookhaven National Laboratory (BNL). Using a pyrolytic graphite (PG) 002 monochromator and analyzer with a mosaic of 24', the neutron energy was set to 14.8 meV ($\lambda = 2.35$ Å). The spectrometer collimation was set at 40'-40'-40'-80'. This yields an instrumental resolution function with a full width at half maximum (FWHM) of 0.04 reciprocal lattice units (RLU) in the scans discussed here, where 1 RLU = $2\pi/a$ and $a = 3.61$ Å. The energy resolution in this configuration (FWHM) is 0.8 meV. In addition, a 50-mm-thick PG filter was used between the sample and analyzer in order to attenuate higher-order neutrons passed by the monochromator. To access a wide range of temperatures, the samples were mounted in a pumped He flow cryostat with a base temperature of 1.4 K.

As shown in the left inset of Fig. 1, Fermi-surface effects such as SDW's are expected to occur at points lying at crossings of arcs with radii $2k_F$ drawn around neighboring Bragg points. This is indeed the case in Cu-

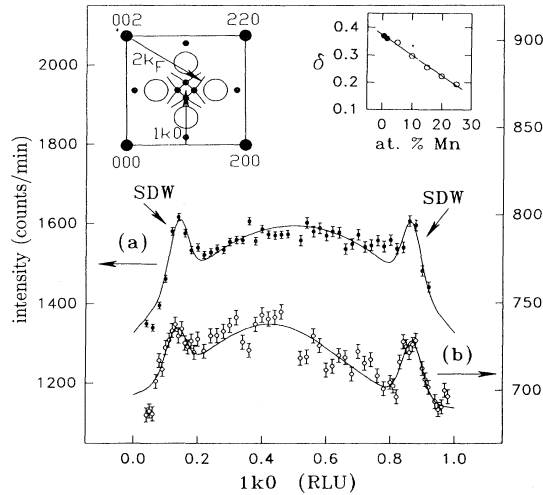


FIG. 1. Elastic neutron-scattering intensities along $1k0$ at $T = 1.4$ K for (a) Cu 1.3% Mn and (b) Cu 0.55% Mn. The counting times per point were 18 min for the 1.3% Mn sample and 44 min for the 0.55% Mn sample. In the inset at the upper left, reciprocal-space positions of incommensurate SDW peaks are shown as small solid circles; commensurate ASRO peaks are shown as large open circles. The $1k0$ scan trajectory is shown by a vertical arrow. In the inset at the upper right, incommensurate SDW peak positions are plotted against Mn composition. The incommensurability parameter δ is defined as 0.5 minus the k value of the first peak shown in the scan trajectory. In RLU, $4k_F^2 = 1^2 + (1.5 - \delta)^2$. Data from Ref. 8 are shown as open circles, while the new data are shown as solid circles.

Mn: SDW features occur in scans along the $1k0$ trajectory shown in the inset. It is readily apparent from Fig. 1 that SDW peaks persist in Cu-Mn alloys containing as little as 0.55% Mn. The solid curves in this figure were generated by fitting the measured data to three Gaussians plus a background. In addition, the central Gaussian for the 0.55% Mn sample was multiplied by a linear function, in order to duplicate the asymmetric shape of the measured peak. Apart from the existence of the SDW peaks, the right-hand inset shows that their positions follow the peak positions found in more concentrated alloys. In other words, in all cases the peaks lie at Fermi-surface crossings.

The temperature dependence of individual SDW features in the two alloys is shown in Fig. 2. The SDW peak intensities obtained by the fitting procedure are shown in Fig. 3. In addition, the intensity of the broad feature at $k = 0.5$ in Fig. 2 was fitted as a function of temperature, in order to generate a temperature-dependent background. For the sample containing 1.3% Mn, only peak intensities were measured at additional temperatures, the background function was subtracted, and these additional points are included in Fig. 3. If the macroscopic magnetic properties in Cu-Mn arise from SDW ordering, then the SDW scattering intensity should act as an order parameter and drop to zero near the spin-glass freezing temperature T_f . Based on magnetic susceptibility measurements,⁷ $T_f \sim 6.5$ K at 0.55% Mn and $T_f \sim 14$

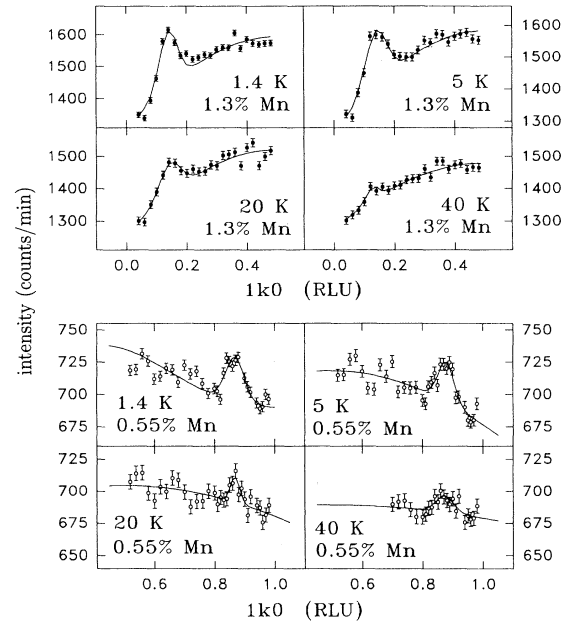


FIG. 2. Temperature dependence of the SDW peaks, for Cu 1.3% Mn (upper plots with solid symbols) and Cu 0.55% Mn (lower plots, open symbols). For the 1.3% Mn sample, the counting times per point were 18 min at $T = 1.4$ K and 9 min at $T = 5, 20,$ and 40 K. For the 0.55% Mn sample, the counting times were 44 min at 1.4 K, 33 min at 5 K, and 22 min at $T = 20$ K and 40 K.

K at 1.3% Mn. However, Fig. 3 shows a slow drop-off in SDW peak intensities as a function of temperature. As discussed previously,^{8,9} this effect is explained as follows. Given the resolution function, in a quasielastic scattering measurement one integrates $S(\mathbf{q}, \omega)$ over a range of ω on either side of $\omega = 0$. If the integrated inelastic scattering is relatively strong in comparison to $S(\mathbf{q}, 0)$ and in addition has a weak temperature dependence, the measured quasielastic scattering can remain significant well above the Néel temperature. For dilute samples,

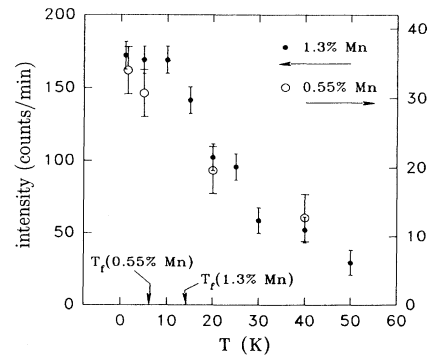


FIG. 3. Temperature dependence of the SDW peak intensities for 1.3% Mn (solid symbols) and 0.55% Mn (open symbols). The intensities used in this plot are primarily derived from Fig. 2, with additional points described in the text.

test measurements with tighter energy resolution are very time-consuming. Nevertheless, it has been shown in more concentrated [15% Mn (Ref. 8) and 8% Mn (Ref. 9)] samples that increasing the ω resolution produces a significantly sharper drop in quasielastic magnetic scattering intensities with increasing temperature.

There are a number of details which are common to all of the neutron data. First, we note that intensities in magnetic scattering are governed by the form factor $f(q)$ of the spin-polarized orbitals. Thus it has not been possible to detect any polarization of Cu conduction electrons, since their wave function is extended and has a form factor which approaches zero starting at very small values of q . Magnetism in the Mn ions, on the other hand, arises in the localized $3d$ orbitals, producing a form factor which falls off relatively slowly. Therefore, magnetic scattering in Cu-Mn alloys serves as a probe of only the Mn spins. It is also clear that the magnetic component of the broad half-integer peak at $k = 0.5$ is ferromagnetic, since it coincides in reciprocal space with an atomic-short-range-order (ASRO) structural peak.¹ In contrast, the incommensurate SDW peaks arise from AFM scattering and are unrelated to structural ordering.¹ Given the nearly linear relation between peak position and Mn concentration (Fig. 1, right inset) the incommensurate peaks are manifestly characteristic of the alloy. They are not due to the formation of stable clusters or other chemical ordering phenomena since in that case the SDW peak *positions* would asymptotically approach a value corresponding to the cluster, rather than directly following the magnitude of the alloy Fermi wave vector k_F . Furthermore, the extrapolated value of the incommensurability parameter δ yields a Fermi-surface diameter in precise agreement with de Haas-van Alphen measurements in pure copper.¹⁰

Before discussing the SDW interpretation of the data, we mention other theories which yield ordering for dilute magnetic systems with *short-range* interactions. Perhaps the simplest such theory is the near-neighbor Ising model worked out originally by Sato *et al.*¹¹ Regardless of the interaction strength, a stable AFM phase results when $cz \geq 2$, where c is the concentration of solute atoms and z is the coordination number. For Cu-Mn, with an exchange coefficient of the appropriate sign, antiferromagnetism would occur at Mn concentrations greater than 16.7%. A similar cutoff occurs with the modified-RKKY-interaction model of Ioffe and Feigel'man.³ Here the Mn-Mn potential is of the form $r^{-1}\sin(2k_F r)e^{-\kappa r}$, which extends beyond near neighbors, bringing the critical concentration of Mn necessary for AFM ordering down to $\sim 10\%$. It has already been pointed out by Cable and Tsunoda¹² that this model is inconsistent with the neutron data for dilute Cu-Mn alloys.

Rather than explicitly working with an interaction potential which is written as a function of the Mn-Mn separation, Fajen and Vignale⁴ start with an interaction which takes place *via* conduction electron polarization:

$$\mathcal{H} = -\frac{G^2}{2L} \sum_{\mathbf{q}} \chi(\mathbf{q}) |\mu(\mathbf{q})|^2, \quad (1)$$

where $\mu(\mathbf{q})$ is the Fourier transform of the distribution of

the L Mn moments in the system and $\chi(\mathbf{q})$ is the susceptibility of the alloy. G is an exchange constant discussed below; its independence from q corresponds to the case of localized Mn spins. Numerical calculations were carried out for Mn concentrations ranging from 0.1% to 5%, utilizing a spin-flipping process to arrive at ground states corresponding to different forms of $\chi(\mathbf{q})$. As in the other models, AFM states were not found when the susceptibility corresponds to the usual RKKY form, that is, for monotonically decreasing $\chi(\mathbf{q})$ (see Fig. 4). However, when a peak in $\chi(\mathbf{q})$ is put in “by hand” at $q = 2k_F$, AFM states emerged at all of the concentrations studied. This result, in parallel with Overhauser’s original considerations,⁶ provides strong evidence that ordered antiferromagnetism in Cu-Mn alloys is stabilized by a peak in $\chi(\mathbf{q})$ at $2k_F$.

In a SDW AFM model of Cu-Mn, one begins by considering the ground state of pure copper. This could be a stable SDW state, but experimental verification of such a state is extremely difficult due to the vanishing form factor discussed above.¹³ Next, consider the case where SDW’s are stabilized by the dilute addition of magnetic ions. This is possible due to the energy gain which is obtained by aligning the solute ions with the local polarization of the SDW, via the *s-d* exchange between the $3d$ Mn electrons and the $4s$ copper conduction band. Apart from neutron-scattering measurements, localization of the magnetic solute orbitals is necessary in order for the SDW phase to be stabilized, since an orbital which extends over an entire oscillation of a SDW has no preferred orientation.¹⁴ Quantitatively, the interaction energy of a magnetic impurity and a SDW is $\mathcal{H}_j = -G(q)\mathbf{S}_j \cdot \hat{\epsilon}P_0\cos(\mathbf{q} \cdot \mathbf{R}_j)$, where $G(q)$ is the exchange constant between isolated spins \mathbf{S}_j and a SDW with wave vector \mathbf{q} and polarization $\hat{\epsilon}$. Mn ions are located at \mathbf{R}_j , and P_0 is the fractional polarization of conduction electrons in the SDW.⁶ The spatial extension of the spins \mathbf{S}_j enters through $G(q)$. After adding the (positive) SDW excitation energy to \mathcal{H}_j , assuming complete alignment of the solute moments, and minimizing with respect to P_0 , the net energy change due to the SDW is

$$\mathcal{H}(\mathbf{q}) = -\left(\frac{2SN_p}{\pi n\mu_B}\right)^2 G^2(q)\chi(\mathbf{q}), \quad (2)$$

where N_p is the concentration of solute atoms, n is the

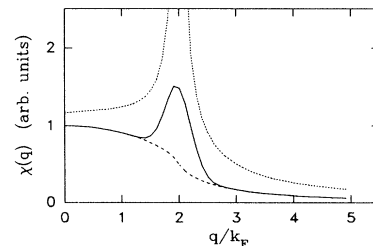


FIG. 4. Schematic plot of the magnetic susceptibility $\chi(\mathbf{q})$, following Refs. 4 and 6. The three qualitative classes of behavior which we consider are a noninteracting electron gas (dashed curve), Coulomb interactions (dotted curve), and an intermediate (partially screened) case (solid curve).

electron density, and μ_B is the Bohr magneton. As in the simulations discussed above,⁴ Eq. (2) implies that an AFM spin state is stabilized by a peak in the susceptibility at nonzero \mathbf{q} . In the original predictions of SDW instabilities by Overhauser,⁶ this peak consists of the singularity at $2k_F$ which is obtained in Hartree-Fock theory of an electron gas with Coulomb interactions. If the electron-electron interaction is completely screened, the singularity and in fact the peak in $\chi(\mathbf{q})$ vanish (Fig. 4). However, as shown by Fajen and Vignale,⁴ a singularity in $\chi(\mathbf{q})$ is not necessary: AFM ordering of magnetic solute atoms occurs when the susceptibility contains a *finite* maximum at a nonzero value of \mathbf{q} .

SDW features occur consistently in neutron-scattering studies of Cu-Mn alloys,^{1,8,12,15,16} with a peak width which is always close to 0.1 RLU, independent of Mn concentration.¹⁷ For SDW antiferromagnetism, this universal width reflects the width of the peak in $\chi(\mathbf{q})$ at $q = 2k_F$. According to the numerical calculations⁴ the width of the peak in $\chi(\mathbf{q})$ is approximately twice the width of the diffraction features. Although neutron count rates have so far prevented significant inelastic studies of samples containing less than 3% Mn, the inelastic fea-

tures for samples containing 3% to 35% Mn are essentially identical: An excitation with a vertical dispersion relation originates at the SDW peak positions. This behavior is characteristic of an excitation originating at the Fermi surface and is highly reminiscent of the behavior in chromium, a prototype SDW AFM.¹⁸ Last of all, there is no sign of a critical Mn concentration which is necessary for other models of AFM ordering. Taken as a whole, the neutron data suggest that the best description of Cu-Mn is a spin-density-wave antiferromagnet, arising from an instability of the electron gas of copper metal at $q = 2k_F$.¹⁹

This work was made possible by NSF Grant No. NSF-PHY 9024608. BNL is supported by DOE Materials Science Contract No. DE-AC0276CH00016. The crystals were grown and analyzed by R. Fiedler, T. J. Gortemulder, A. A. Menovsky, and C. E. Snel. Measurements at H7 were performed with the essential assistance of R. Rothe, R. Liegel, and J. Biancarosa. Finally, we acknowledge very useful discussions with G. Vignale, G. Shirane, B. J. Sternlieb, and A. W. Overhauser.

*Present address: Department of Physics, Marquette University, Milwaukee, WI 53233.

¹J. W. Cable, S. A. Werner, G. P. Felcher, and N. Wakabayashi, *Phys. Rev. B* **29**, 1268 (1984).

²Earlier neutron-scattering measurements focused on clustering and relaxation phenomena. See, for example, A. P. Murani, *Phys. Rev. Lett.* **41**, 1406 (1978).

³L. B. Ioffe and M. V. Feigel'man, *Sov. Phys. JETP* **61**, 354 (1985).

⁴O. Fajen and G. Vignale, *Solid State Commun.* **77**, 829 (1991).

⁵K. Binder and A. P. Young, *Rev. Mod. Phys.* **58**, 801 (1986).

⁶A. W. Overhauser, *Phys. Rev.* **128**, 1437 (1962).

⁷J. A. Mydosh, *Spin Glasses: An Experimental Introduction* (Taylor & Francis, London, 1993).

⁸S. A. Werner, J. J. Rhyne, and J. A. Gotaas, *Solid State Commun.* **56**, 457 (1985).

⁹A. P. Murani and A. Heidemann, *Phys. Rev. Lett.* **41**, 1402 (1978).

¹⁰D. Shoenberg, *Philos. Trans. R. Soc. London A* **255**, 85 (1962); D. J. Roaf, *ibid.* **255**, 135 (1962).

¹¹H. Sato, A. Arrott, and R. Kikuchi, *J. Phys. Chem. Solids* **10**, 19 (1959).

¹²J. W. Cable and Y. Tsunoda, *J. Appl. Phys.* **73**, 5454 (1993).

¹³A preliminary search for SDW features in pure Cu has yielded a null result: S. A. Werner, J. M. Tranquada, and G. Shirane (unpublished).

¹⁴This was originally pointed out by A. W. Overhauser, *J. Phys. Chem. Solids* **13**, 71 (1960).

¹⁵Y. Tsunoda, N. Kunitomi, and J. W. Cable, *J. Appl. Phys.* **57**, 3753 (1985).

¹⁶Y. Tsunoda and J. W. Cable, *Phys. Rev. B* **46**, 930 (1992).

¹⁷An exception with rather sharp diffraction peaks is found in Ref. 16, consisting of a highly concentrated (35% Mn) sample which was subjected to prolonged low-temperature anneals in order to develop ASRO. This sample clearly belongs in a different class than the typical Cu-Mn alloys. Interestingly, SDW peaks with the usual width show up in the *inelastic* scans on this sample.

¹⁸Eric Fawcett, *Rev. Mod. Phys.* **60**, 209 (1988).

¹⁹Samuel A. Werner, *Comments Condens. Matter Phys.* **15**, 55 (1990).